ChemComm

Accepted Manuscript

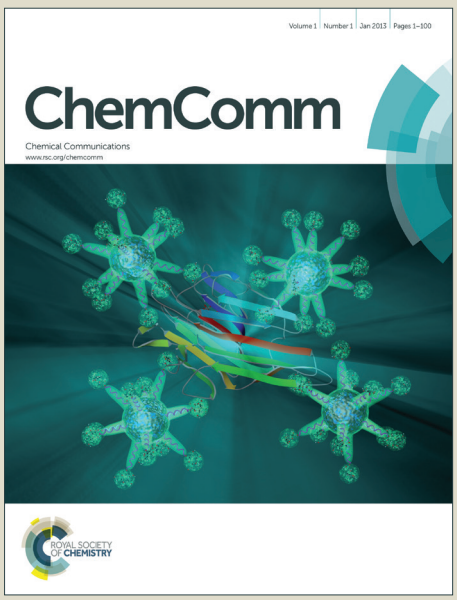

ROYAL SOCIETY OF CHEMISTRY

www.rsc.org/chemcomm

Cite this: DOI: 10.1039/c0xx00000x

www.rsc.org/xxxxxx

ARTICLE TYPE

In situ helicity inversion of self-assembled nano helices

Rumi Tamoto,[a] Nicolas Daugey,[b] Thierry Buffeteau,[b] Brice Kauffmann,[c] Makoto Takafuji,[d] Hirotaka Ihara[d] and Reiko Oda*[,a]

Received (in XXX, XXX) Xth XXXXXXXXX 20XX, Accepted Xth XXXXXXXXX 20XX

DOI: 10.1039/b000000x

The handedness of nanometrical helices based on surfactant assemblies was inverted when these helices were in contact with the excess solution of chiral anions with opposite enantiomers. An important difference in the kinetics of chirality inversion at molecular level and mesoscopic level was observed.

Most biological macromolecules such as proteins and nucleic acids are optically active and adopt one-handed helices. Their structures play an important role in their inter/intra molecular interactions and functions. Recently, there are many reports on biologically inspired synthetic helical structure obtained by oligomers, polymers, foldamers and self-assembled low molecular weight molecules. The helices with controllable pitches are attractive not only to mimic nature, but also for the wide range of applications in materials sciences, chemical and biomaterial sensing, and enantioselective catalysis.[1] The primary advantage of these synthetic structures lies in the ability to control the expressed chirality. Supramolecular helices can express the chirality with specific handedness which depends on the molecular chirality, and the expressed chirality at mesoscopic level is around nanometer to micrometer,[2] indicating the intimate association between molecular chirality with the growth and stability of self-assembled chiral fibers. Mostly, the driving force for the helical structures originates from delicate balance between inter/intramolecular π-stacking, steric hindrance and hydrogen bond interaction.[3]

The chirality inversions in helical structures are known both in nature and in the synthetic systems. A right-handed helical protein or polymer chains can organize into a left-handed helical superstructure,[4,5] Many macromolecules are reported to change their helicity between *P* and *M* in a so-called helix-helix transition by applying an external stimulus such as light,[6] solvent,[7] temperature,[8] pH value,[9] and chiral and/or small molecule additives via host-guest interaction.[10] Most of these examples of chirality inversion concern the helical organization of macromolecules/foldamers at the molecular or supramolecular level, and the chirality is expressed at nanometer level. These molecules with controllable helicity exhibit optical activity and inversion steps can be demonstrated by chiroptical spectroscopic methods. Due to their small size, the morphologies and the kinetics of these helices can mainly be followed by spectroscopic techniques such as CD, NMR, Fluorescence or UV or X-ray crystallography.[11] Only a few examples are found in the literature about helical inversion on molecular assembly systems,[12,13] and the kinetic aspects of these inversion are rarely discussed. Herein, we present a system based on chiral supramolecular structures in which we can directly visualize ambiguously step by step *in situ* helicity inversion for the first time at sub-micron level.

Previously, we reported that chiral supramolecular nanostructures can be achieved from non-chiral cationic surfactants with chiral counterions tartrate in water or organic solvents.[14,15,16] Various chiral structures such as twisted, helical, and tubular nanostructures with controllable chirality are observed. These surfactants, called gemini surfactants, are formed with two symmetrical 16 carbon chains with two hydrophilic heads (quaternary ammoniums) connected by an ethylene spacer, denoted as 16-2-16. In contrast to chiral polymers, these molecular assembly structures are based solely on molecular assemblies with non-covalent interaction, and on the stacking of bilayers with well-ordered crystalline organization both of surfactants, counterions and water. Their morphologies are controlled by parameters such as temperature, additives, enantiomeric excess (ee), but also the aging factor turned out to be crucial.[17] Various morphologies with finely tunable shapes are observed as a function of ee. Flat ribbons are observed with racemic mixture of L-tartrate: D-tartrate (1 : 1). With increasing ee, twisted ribbons with decreasing pitches are observed, and for ee ~ 1, helical ribbon, and tubules are observed. For ee ~ 1, tubules transform to twisted ribbons upon heating, or with a small quantity of additives. Finally, twisted ribbons transform to helical ribbons then to tubules upon aging of the assemblies.**Error! Bookmark not defined.**

The originality of this system is that the chirality is introduced by the counterions *via* electrostatic interaction and not covalent attachment to membrane forming moieties, i.e. gemini surfactants. This property allows us to access an extremely interesting observation reported here: the mesoscopic chirality (helicity) of these molecular assemblies with tens to hundreds of nanometers can be inverted *in situ* in solution at constant temperature, by introduction of opposite chiral acid (D-tartaric acid) into the gel network formed with nanometric helices of 16-2-16 L-tartrate. This induces the ion exchange at the surface of charged bilayers, and final enantiomeric excess of the system is modified as a function of the quantity of the added D-tartaric acid. Due to their relatively "large" size, we succeeded in visualizing and following the mesoscopic helicity inversion using transmission electron microscopy (TEM) while the process of molecular chirality transfer was followed by circular dichroism

(CD) and Raman optical activity (ROA) and molecular organization by Small Angle X-ray Scattering (SAXS).

The 16-2-16 L-tartrate forms gel with *P* tubular structures in water. On this gel (10 mM), D-tartaric acid solutions with various equivalences of D-tartrate (1 eq, 2 eq, 4 eq, and 20 eq) were poured through, then the gel was then rinsed with a large amount of milli-Q water, then the structural variation of the gel was followed with time.

At first, we followed the morphology transformation using TEM with 1 equivalent of D-tartaric acid solution (ee =0). Just after rinsing, the *P* tubular fibers of 16-2-16 L-tartrate (Figure 1 a) were slowly unwound to *P* helical structures (Figure 1 b1), which transformed to twist ribbons within a few hours (Figure 1 b2). Their twist pitches increased to micrometric scale and a mixture of flat ribbons with some long pitch *P* and *M* twist ribbons were observed after one day (Figure 1 b3, b4).

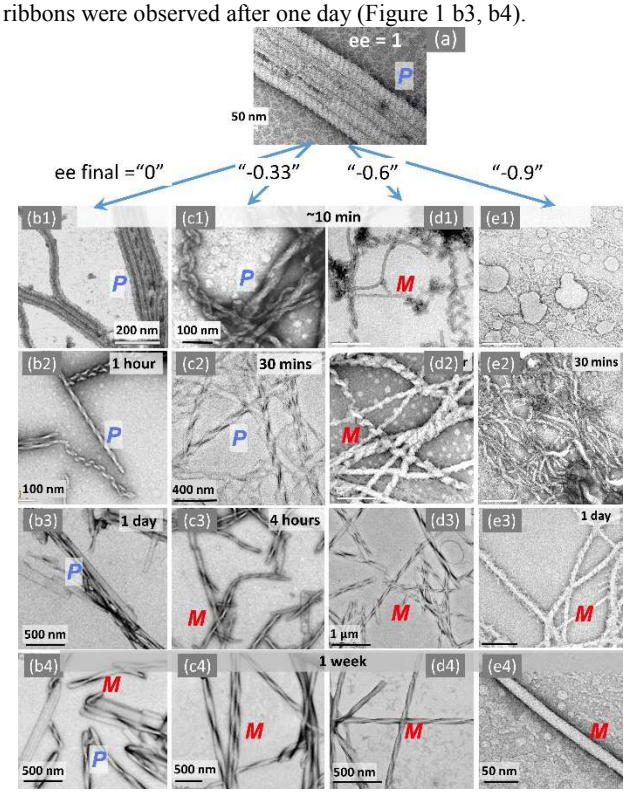

Figure 1. TEM images of morphology transformation of *P* tubes from 16-2-16 L-tartrate with pure enantiomer (a, ee = 1) with different ee changes (b, ee=0; c, ee=-0.33; d, ee=-0.6 and e, ee=-0.9) by filtration of opposite chiral D-tartaric acid solution through the 16-2-16 L-tartrate gel.

For two equivalence of D-tartaric acid solution (ee =-0.33), unfolded *P* helical ribbons were observed during the first hour (Figure 1 c1, c2). After 1 hour, only *M* helical ribbons with tight pitches were observed (Figure 1 c2), which transformed into twisted ribbons with increasing pitch and reached the equilibrium value after about one day. With 4 equivalence of D-tartaric acid (ee =-0.60) solution, the *P* tubular fibers immediately transformed to *M* helical ribbons with small pitches (Figure 1 d1). Interestingly, these *M* helical structures transformed to twisted ribbons with larger pitches (a few hundred nanometers) after 1 week (Figure 1 d4). On the macroscopic aspect, initially all above samples were translucent solution, and then turned into cloudy gel after about 1 hour. Finally, when a large excess of D-tartaric acid (20 equivalents, ee = -0.90) was added, the fiber structures collapsed immediately to form spherical structures (Figure 1 e1). They reassembled to *M* helical ribbons after 30 minutes (Figure 1 e2), then left handed *M* helices after a day, (Figure 1 e3) then into tubular structures after one week (Figure 1 e4).

In order to obtain the insight on the chirality inversion at the molecular level, the helicity inversion process was monitored by chiroptical spectroscopic techniques. The change of the chiral anions in the gel was followed by electronic circular dichroism (CD), whereas the inversion of the helicity of surfactant bilayers was evidenced by Raman optical activity (ROA).

As we have previously demonstrated, a strong exciton coupling between carboxylate groups of tartrate is observed with a positive peak at 201 nm and a negative peak at 217 nm for 16-2-16 L-tartrate gels (green spectra in Figure 2). The effect of enantiomeric excess on the chiroptical properties of the gels have already been demonstrated.[18] Decreasing ee caused non-linear decrease of the intensity of the cotton coupling between the carboxylates. Figure 2 shows the variation of CD signals after filtration of D-tartaric acid. As it is clearly seen, the CD signals change immediately (within minutes) for all cases.

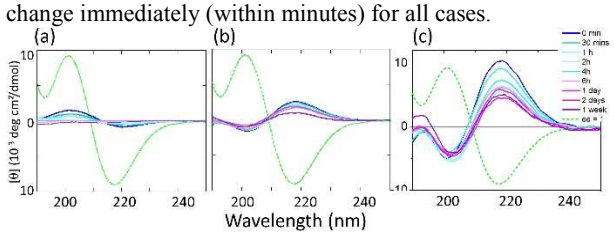

Figure 2. CD spectra of 16-2-16 tartrate with different ee changes: (a) 0, (b) -0.60, and (c) -0.90

For ee=0 immediately after the filtration of D-tartaric acid solution, the intensity of the two bands at 201 nm and 217 nm decreased quickly to about 15% of the original intensity and totally disappeared after 4 h (Figure 2a). It is noteworthy that at this point, the TEM images still show the presence of twisted ribbons with long pitch (≥ 1000 nm). For ee=-0.33, -0.6 (Figure 2b) and -0.90 (Figure 2c) the signs of CD bands at 201 nm and 217 nm were immediately inverted. These peaks decreased with time to about 50-70 % of their initial intensities until they were stabilized after few hours. Figure 3 (a) and (b) compare the variation of the twist pitch and the difference of CD intensities for the two bands with time after the addition of D tartaric acid for different final ee's. This figure clearly shows the strong correlation between the morphologies of chiral fibers as observed by TEM image and the molecular chirality observed with CD signals. A detailed analysis of the kinetics of the two data sets shows however, that the variation of the CD signal is much more rapid than the morphology variation. These phenomena suggest that the counter-anions on self-assembled amphiphiles were exchanged rapidly from L-tartrate to D-tartrate, but the resulting structural helicity inversion is much slower.

We also probed the kinetics of supramolecular organization during morphology transition using small angle X-ray scattering (SAXS). The evolution of the full width at half maximum (FWHM) of the correlation peak observed by SAXS around 0.185 $Å^{-1}$, characteristic of a repeat distance of molecular packing of 34 Å, is shown in Figure 3(c). For ee=1, a broad correlation peak is observed (supporting information). Upon addition of D-tartaric acid, these peaks transform to fine peaks. For ee=0, this transition is relatively quick (after 30 minutes). For ee=-0.33, the transformation to fine peaks is slower, e.g. 2-3 hours. For ee=-0.9, the correlation peak disappears after 30 minutes, then reappear again after 1.5 hours. These results agree also with TEM observations, namely the unwinding and formation of multilayer ribbons for ee=0, of oppositely twisted ribbons for ee=-0.33 after

a few hours, and the disappearance of ribbons first, then their re-formation with opposite handedness after an hour for e=-0.9.

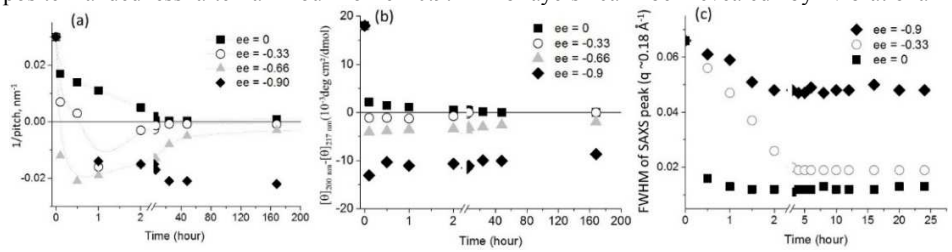

Figure 3. Evolution of (a) twist pitches periods and (b) difference of CD intensities for the two bands at 201 nm and 217 nm, and (c) FWHM of SAXS peak at q~0.185 Å^{-1}.with various ee from 1 to 0, 1 to -0.33, 1 to -0.60 and 1 to -0.90 by filtration of opposite chiral D-tartaric acid solution through the 16-2-16 L-tartrate gel.

Previously, we have shown that the chirality of the surfactant bilayers can be revealed by vibrational circular dichroism (VCD).[18,19] Here, we used the Raman optical activity (ROA), which is also sensitive to the amphiphilic moieties of the molecule. Figure 4 shows the ROA spectra in the 1800-800 cm^{-1} spectral range before (Figure 4a) and, at different times (Figures 4b to 4g), after filtration of 20 eq of D-tartaric acid into a 10 mM 16-2-16 L-tartrate gel and rinsing with water. ROA contributions are observed around 1450 cm^{-1} and at 1172 and 1138 cm^{-1} assigned to the bending (δCH_2) and rocking (ρCH_2) vibrations of the long chain methylene groups and to the symmetric stretching (ν_sC-C) vibration of the carbon backbone, respectively.[19]

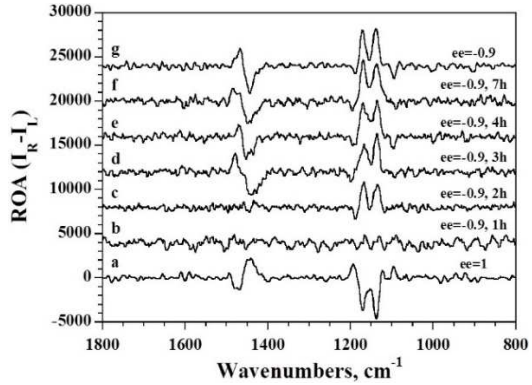

Figure 4. ROA spectra of 16-2-16 tartrate amphiphiles (10 mM) for ee=1 and for ee=-0.9 after addition of opposite chiral D-tartaric acid solution through the 16-2-16 L-tartrate gel.

The ROA spectrum recorded one day after the counterion exchange (Figure 5g) show sign inversion (Figure 4a), revealing the chirality inversion of the surfactant bilayers. The more detailed analysis of the spectra revealed interesting kinetic characteristics. During the first hour after the counterion exchange, no ROA contribution was observed (Figure 4b), suggesting that the chiral structures of the fibers were destroyed just after addition of D-tartaric acid, in agreement with the TEM observation. The maximum intensity of the ROA signal is recovered after few hours (5-7 hours).

In order to correlate the data from TEM, CD, ROA, and SAXS, it is important to understand what happens during the chirality inversion at molecular level. For this, we recall some features of the detailed molecular organization model that we have reported previously, using 16-2-16 racemate tartrate self-assembled multi-bilayer ribbons based on X-ray diffraction, vibrational circular dichroism, and molecular modelling.**Error! Bookmark not defined.**[20] The dications in the head group of gemini amphiphiles composed of N^+-C-C-N^+ are intrinsically achiral but adopt two mirror-image conformations at their head groups. According to the planar chiral shape of the ethylene spacer from a top view, these conformations are noted Z and backwardZ, and both conformations are found in the ribbons. L or D tartrate has specific interaction with the same gemini molecule taking one of the two conformations Z or backwardsZ.[20] Our analysis showed that there are **two heterochiral bilayers** per unit cell, comprised of homochiral monolayers, in which each gemini conformation has stronger affinity with one of the two enantiomers of tartrate. This organization is conserved through large morphology transitions from racemic, flat multilayered ribbons to chirally twisted, helical ribbons as well as tubules of the pure enantiomer. The detailed analysis of the ensemble of these results indicated that every monolayer is homochiral formed with gemini with homogeneous Z or backwardZ conformation complexed with D or L tartrate, and the other monolayer of the same bilayer is composed of gemini and tartrate of opposite chirality (heterochiral bilayer) (Figure 5). In the case of a pure enantiomer (L for instance), only two bilayers can stack, with four monolayers (see Figure 5, ee=1). The two internal monolayers share the same chirality, for example L-backwardZ - L-backwardZ array of headgroups and tartrate ions. If the conformation of the internal monolayers is backwardZ, the heterochiral bilayer packing requires that the gemini conformation of the external leaflets of these double-bilayer ribbons is Z, and obviously, the only available tartrate (L) cannot be accommodated within the chiral cavity where D tartrates are expected. Based on this analysis, the number of bilayers can be calculated to be as 2/ee. Indeed, for ee=1, there are two bilayers, ee=0.5, 4 bilayers …, which agrees well with the TEM observation (supporting information)

These insights into the molecular-scale packing within membrane ribbons shed light on a number of macroscopic features and their kinetics. In the present case, when 1 to 4 equivalents of D-tartaric acid is added to 16-2-16 L-tartrate gel network, the D-tartrate ions fill the cavities in the outer layer with Z conformation. Consequently, it allows the stacking of multi-bilayers to continue having D-Z and L-backwardZ formations, which could lead from double-bilayer tubular structure to multi-bilayer ribbons (SAXS peak refining due to stronger structure factor contribution). Since, globally D tartrate will be the majority, the inversion of the D-L ratio in the ribbons will occur (CD signal inversion) along with the continuous helicity inversion of the ribbons (TEM). In contrast, when 20 equivalents D-tartaric acid is added, the large excess of D-tartrate ions interact directly both with the outer layer with Z conformation and the inner later with backwardZ layer (CD signal inversion). Consequently, double-bilayers along with fiber are destroyed

during counter-anion exchange just after addition of D-tartaric acid. Then the molecular re-assembling occurs with D-Z and D-backwardZ double-bilayer formation. (TEM, SAXS, ROA).

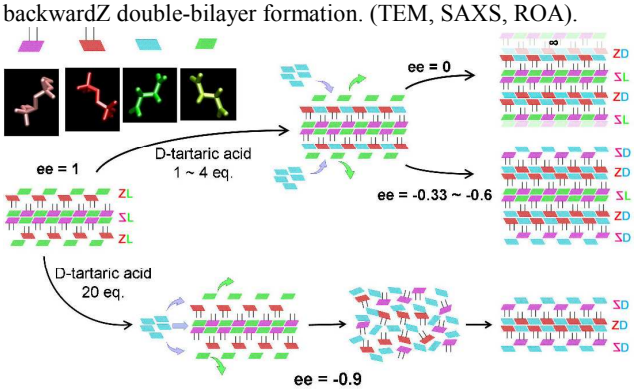

Figure 5. Schematic illustration of the change of molecular organization during morphology transformation. The pink and red symbols represent the two conformations of gemini molecules, backwardZ and Z, blue and green symbols are D and L tartrate.

In Conclusion, we succeeded in visualizing the *in situ* chirality inversion of self-assembled helices in aqueous solution. This inversion is induced simply by the addition of tartaric acid solution of the opposite enantiomer to the helix suspension of 16-2-16 tartrate. It was clearly observed that this helix inversion is the cooperative result of various transitions, from molecular to mesoscopic scale, with different kinetics: the chirality inversion of tartrate anions, as observed by CD, occurs very quickly. Indeed, by the time it took us to add the acid, rinse it, and measure the CD signals (about 10 minutes), CD signals were inverted for all the samples with ee≠0. The counterion exchange is immediate when the aggregates are in contact with the opposite enantiomers. Meanwhile, the organization of the gemini, as observed by ATR or SAXS, takes longer (a few hours). This molecular organization accompanies the helicity inversion. For ee=-0.9, the initial fibers are destroyed in the first hour before the reformation of fibers with opposite helicity, as observed by TEM and ROA. Morphological helicity inversion process is slow, of the order of the days. This study clearly elucidates for the first time, the multi-step mechanisms in the chirality inversion of molecular aggregates. This work was supported by French CNRS and Université de Bordeaux. We thank Japan Student Services Organization for the PhD student fellowship.

Notes and references

[a] *Institute of Chemistry & Biology of Membranes & Nanoobjects, CNRS – Université de Bordeaux, UMR5248, 2 rue Robert Escarpit, 33607, Pessac, France. Tel: +33 54000* 2229; r.oda@cbmn.u-bordeaux.fr
[b] *Institut des Sciences Moléculaires, CNRS-Université de Bordeaux UMR 5255, 351 Cours de la Libération, 33405, Talence, France. Tel: +33 54000 6365; t.buffeteau@ism.u-bordeaux1.fr*
[c] *Institut Européen de Chimie et Biologie, 2, Rue Robert Escarpit, 33607 Pessac, France, Tel: +33 54000 3054; b.kauffmann@iecb.u-bordeaux.fr*
[d] *Department of Applied Chemistry and Biochemistry, Kumamoto University, 2-39-1, Kurokami, Kumamoto 860-8555, Japan Tel:+81 96-342-3663 ihara@gpo.kumamoto-u.ac.jp, takafuji@kumamoto-u.ac.jp*

† Electronic Supplementary Information (ESI) available: [details of any supplementary information available should be included here]. See DOI: 10.1039/b000000x/

[1] E. Yashima, *Analytical Sciences*, 2002, **18**, 3-6.
[2] (a) D.A. Frankel, D. F. O'Brien, *J. Am. Chem. Soc.*, 1994, **116**, 10057 (b) E. Yashima, T. Matsushima, Y. Okamoto, *J. Am. Chem. Soc.*, 1997, **119**,6345.(c) J. J. L. M. Cornelissen, M. Fischer, N. A. J. M. Sommerdijk, R. J. M. Nolte, *Science*, 1998, **280**, 1427. (d) J. H. K. K. Hirschberg, L. Brunsveld, A. Ramzi, J. A. J. M. Vekemans, R. P. Sijbesma, E. W. Meijer, *Nature*, 2000, **407**, 167. (e) M. Fujiki, *Macromol. Rapid Commun.*, 2001. **22**,539.
[3] (a) J. P. Hill, W. Jin, A. Kosaka, K. Fukushima, H. Ichihara, T.Shimomura, K. Ito, K. Hashizume, N. Ishii, T. Aida, *Science*, 2004, **304**, 1481. (b) F. J. M. Hoeben, P. Jonkheijm, E. W. Meijer, A. P. H. J. Schenning, *Chem.Rev.*, 2005, **105**, 1491. (c) W. Jin, T. Fukushima, M. Niki, A. Kosaka, N. Ishii, T. Aida, *Proc. Natl. Acad. Sci. USA*, 2005, **102**, 10801. (d) A. Ajayaghosh, R. Varghese, S. J.George, C. Vijayakumar, *Angew. Chem.*, 2006, **118**, 1159.(e) Y. Yan, K. Deng, Z. Yu, Z. Wei,*Angew. Chem.*, 2009, **121**,2037.
[4] V. N. Malashkevidh, R.A. Kammerer, V.P. Efimov, T. Schulthess, J.Engel, *Science*, 1996, **274**, 761.
[5] J. J. L. M. Cornelissen, M. Fischer, N. A. J. M. Sommerdijik, R. J. M. Nolte, *Science*, 1998, **280**, 1427.
[6] (a) G. Maxein, R. Zentel, *Macromolecules*, 1995, **28**, 8438. (b) Q. Li, L. Green, N. Venkataraman, I. Shiyanovskaya, A. Khan, A. Urbas, J. W. Doane, *J. Am. Chem. Soc.* 2007, **129**, 12908.
[7] (a) B. M. W. Langeveld-Voss, M. P. T. Christiaans, R. A. J. Janssen, E. W. Meijer, *Macromolecules*, 1998, **31**, 6702. (b) H. Goto, Y. Okamoato, E. Yashima, *Macromolecules*, 2002, *35*, 4590. (c) W. Peng, M.Motonaga, J. R. Koe, *J. Am.Chem. Soc,* 2004, **126**, 13822 (d) S. Sakurai, K. Okoshi, J. Kumaki, E. Yashima, *J. Am. Chem. Soc,* 2006, **128**, 5650.
[8] (a) J. R. Koe, M. Fujiki, M. Motonaga, H. Nakashima, *Chem. Comm*, 2000, 389.(b) M. Fujiki, *J. Am. Chem. Soc.,* 2000, **122**, 3336. (c) T. Hasegawa, K. Morino,Y. Tanaka, H. Katagiri, Y. Furusho, E. Yashima, *Macromolecules*, 2006, **39**, 482.(d) K. Nagai, K. Maeda, Y. Takeyama, T. Sato, E. Yashima, *Chem Aian J.*, 2007, **129**, 12908 (e) N. Delsuc, T. Kawanami, J. Lefeuvre, = A. Shundo, H. Ihara, M. Takafuji, I. Huc, *ChemPhysChem*, 2008, **9**, 1882.(f) M. Banno, T. Yamaguchi, K. Nagai, C. Kaiser, S. Hecht, and E. Yashima, *J. Am. Chem. Soc.*, 2012, **134**, 8718
[9] Y. Li, H. Wang, L. Wang, F. Zhou, Y. Chen, B. Li, Y. Yang, *Nanotechnology*, 2011, **22**, 135605.
[10] (a) E. Yashima, Y. Maeda, Y. Okamoto, *J. Am. Chem. Soc.,* 1998, **120**,8895.(b) K. Morino, K. Maeda, E. Yashima, *Macromolecules*,2003, **36**, 1480. (c) E. Yashima, K. Maeda, Y. Furusho, *Acc. Chem. Res.*, 2008, **41**, 1166. (d) B. Prince, S. A. Barnes, J. S. Moore, *J. Am. Chem. Soc.* 2000, *122*, 2758. (e) Q.Gan, Y. Ferrand, N. Chandramouli, B. Kauffmann, C. Aube, D. Dubreuil, I. Huc *J. Am. Chem.Soc.* 2012, **134**, 15656. (f) H. Miyake, K. Yoshida, H. Sugimoto, H. Tsukube, *J Am Chem Soc.* 2004, **126**, 6524.
[11] G. A. Hembury, V. V. Borovkov, Y. Inoue, Chem. Rev.2008, **108**, 1
[12] R. S. Johnson, T. Yamazaki, A. Kovalenko, H. Fenniri, *J. Am. Chem. Soc.,* 2007, **129**, 5735.
[13] Y. Huang, J. Hu, W. Kuang, Z. Wei, C. F. J. Faulc, *Chem. Commun.* 2011, **47**, 5554.
[14] R. Oda, I. Huc, S. J. Candau, *Angew. Chem. Int. Ed.*, 1998, **37**, 2689
[15] R. Oda, I. Huc, M. Schmuts, S. J. Candau, F. C. Mackintosh, *Nature*, 1999, **399**, 566.
[16] R. Oda, in *Molecular Gels* Kluwer Academic Publishers, Dordrecht, The Netherlands 2005. Weiss, Richard G., Terech, Pierre (Eds.)
[17] A. Brizard, C. Aimé, T. Labrot, I. Huc, D. Berthier, F. Artzner, B. Desbat, R. Oda, *J. Am. Chem. Soc.,* 2007, **129**, 3754.
[18] (a) D. Berthier, T. Buffeteau, J. M. Léger, R. Oda, I. Huc, *J. Am. Chem. Soc.*, 2002, **124**, 13486. (b) A. Brizard, D. Berthier, C. Aimé, T. Buffeteau, D.Cavagnat, L. Ducasse, I. Huc, R. Oda, *Chiraliy*, 2009, **21**, 153.
[19] P. J. Hendra, H. P Jobic, E. P. Marsden, D. Bloor, *Spectrochimica Acta*, 1977, **33A**, 445.
[20] R. Oda, F. Artzner, M. Laguerre, I. Huc, *J. Am. Chem. Soc.*, 2008, **130**, 14705